

SEVENTH EUROPEAN ROTORCRAFT AND POWERED LIFT AIRCRAFT FORUM

Paper No. 38

A CONTROL MODEL FOR MANEUVERING FLIGHT FOR  
APPLICATION TO A COMPUTER-FLIGHT-TESTING PROGRAM

H. Haverdings

National Aerospace Laboratory NLR  
Amsterdam, The Netherlands

September 8-11, 1981

Garmisch-Partenkirchen  
Federal Republic of Germany

Deutsche Gesellschaft für Luft- und Raumfahrt e. V.  
Goethestr. 10, D-5000 Köln 51, F.R.G.

A CONTROL MODEL FOR MANEUVERING FLIGHT  
FOR APPLICATION TO A COMPUTER-FLIGHT-TESTING PROGRAM

H. Haverdings

National Aerospace Laboratory NLR

ABSTRACT

A computer-flight-testing (CFT) program for helicopters has been under development at NLR for some time to evaluate helicopter dynamics and handling and control qualities. To eliminate problems in estimating control inputs during maneuvering flight, the nonlinear 6 degrees of freedom helicopter model is driven by control inputs generated by a specially developed control model (or "pseudo pilot"). This is an adaptation of a linear optimal control model as used in human factor analysis.

The helicopter model is based on 2-dim. strip aerodynamics and steady-state rotor blade dynamics using only out-of-plane bending mode shapes, which are suitable for various types of rotor articulation.

The "pilot" model consists of a flight path generation (FPG)- model and a stabilization (STAB)- model. The FPG-model is based on linearized system dynamics using terminal optimal control, generating both the required flight path and the control inputs to achieve it. These controls are input into the helicopter model. The two flight paths are compared, and differences are fed back to the STAB-model to generate corrective control inputs of such a nature that the helicopter-model-generated flight path tracks the required flight path generated by the FPG-model. Also the STAB-model is based on linearized system dynamics.

As an example, two flare maneuvers are "flown", and the results discussed. The pseudo-pilot model performs well, provided that helicopter dynamics do not change much during a specific maneuver.

LIST OF SYMBOLS

A	system dynamics matrix, eq. (3.1)		
B	control distribution matrix, eq. (3.1)	$\underline{u}_s$	stability control vector, eq. (3.1)
$\underline{c}$	terminal condition vector, eq. (3.8)	$\underline{u}_t$	total control vector, eq. (2.3)
$\underline{f}$	forcing vector, eq. (2.1)	$\underline{u}_d$	desired control vector, eq. (3.5)
$f_n$	rotor blade forcing function, eq. (2.4)	V	aircraft inertial velocity, eq. (2.7) (a), m/s
F	system dynamics matrix, eq. (3.5)	v	component of inertial velocity along Y-axis of aircraft, positive to the right, m/s
G	control distribution matrix, eq. (3.5)	w	component of inertial velocity along Z-axis of aircraft, positive downward, m/s
$\underline{g}$	augmented forcing vector function, eq. (2.9)	x	distance travelled along direction of earth-oriented X-axis, positive forward, m
H	terminal condition distribution matrix, eq. (3.8)	$\underline{x}_d$	desired state vector, eq. (3.5)
$\underline{h}$	prescribed time vector function, eq. (3.10)	$\underline{x}_s$	stability state vector, eq. (3.1)
h	altitude, element of state vector, m	$\underline{x}_t$	total state vector, eq. (2.2)
$J_s$	performance index for stabilization, eq. (3.3)	$\hat{\underline{x}}_t$	augmented total state vector, eq. (A.1)
$J_d$	performance index for maneuver, eq. (3.9)	$\hat{\underline{x}}_t$	estimate of $\hat{\underline{x}}_t$ , eq. (A.2)
k	number of blade mode shapes	y	distance travelled along earth-oriented Y-axis, positive to the right, m
L	feedback gain matrix, eq. (3.4)	$\delta_a$	lateral control stick displacement, percent from full left
M(t)	mass and inertia matrix, eq. (2.1)	$\delta_{CP}$	collective pitch lever displacement, percent from full up
p	aircraft roll rate, positive to the right, rad/s	$\delta_e$	longitudinal control stick displacement, percent from full forward
$Q_x$	weighting matrix on the state, eq. (3.3)	$\delta_r$	rudder pedal displacement, percent from full left
$Q_u$	weighting matrix on the control, eq. (3.3)	$\theta$	aircraft pitch angle, positive nose up, rad
$Q_{\dot{u}}$	weighting matrix on control rate, eq. (3.3)	$\lambda_n$	nth bending mode eigenfrequency ratio
q	aircraft pitch rate, positive nose up, rad/s	$\phi$	aircraft roll angle, positive "right wing" down, rad
$q_n$	rotor blade $n^{\text{th}}$ modal displacement, eq. (2.4)	$\psi$	aircraft azimuth angle, positive nose to the right, rad
$q_{n_o}$	Fourrier coefficients of $q_n$ , eq. (2.5)	$\psi$	rotor blade azimuth angle, positive for anti-clockwise rotation, rad
$q_{n_c}$		$\Omega$	rotor rotational speed, rad/s
$q_{n_s}$		(.)	= d( )/dt, time derivative
r	aircraft yaw rate, positive nose right, rad/s	( )'	= d( )/d $\psi$ , blade azimuth derivative
ROC	aircraft rate of climb, m/s		
s	Laplace variable		
t	time, s		
$T_N$	neuro-muscular lag matrix, eq. (3.4)		
$t_f$	final time, s		
u	component of inertial velocity along X-axis of aircraft, positive forward, m/s		

## 1 INTRODUCTION

A Computer-Flight-Testing (CFT-) program for helicopters has been under development at NLR for some time. With this program, dynamic aspects of helicopter flying can be calculated or simulated under various conditions of helicopter configuration and atmospheric circumstances. Typical applications might entail the following:

- determination of aircraft gust response
- determination of maneuver loads
- study of minimum distance to clear an obstacle
- examination of large-perturbation response to control inputs and external perturbations
- determination of thrust and power maneuver limits
- simulation of tactical maneuvers
- determination of total aircraft stability, including the studying of time histories.

Two operating parts of the computer program may be discerned, viz. a static (or trim) part, and a dynamic part. The first part is used to calculate the trim values of various helicopter parameters such as control positions, the attitude of the fuselage, rotor blade coning and flapping, and trim forces and moments acting on rotors and fuselage. The second part calculates the time histories of the helicopter motion variables as result of: control inputs, gust inputs, recoil forces from on-board weapons and change of helicopter mass and/or c.g. location.

When a specific maneuver is required, e.g. a landing flare or a transition from hover to level flight the user of the CFT-program, before the controller had been developed, had to supply the time histories of the various controls (longitudinal and lateral cyclic control, collective control, rudder pedal) to effect the required maneuver. In practice this turned out to be a very difficult task, especially when it was required to maintain heading, keep altitude constant, or the like. The matching of the 4 controls in synchronization so as to execute the maneuver at hand proved to be almost impossible, especially when no prior information from actual flight tests was available. To alleviate this problem a controller was designed and implemented in the CFT-program, enabling various types of maneuvers to be made, meeting prescribed terminal conditions at a specified final time.

The theoretical basis of the controller is rooted in optimal control theory as applied to linear(ized) dynamical systems. There are connections with human factor analysis work, in that the controller, in the application to the CFT-program, may be regarded as a highly motivated, well-trained pilot having perfect information about the entire state of the helicopter. In mathematical terms this means that perfect observations of the entire helicopter state are made, but that there are time delays when applying corrective control inputs. These time delays reflect the neuro-muscular lags of the human, or his reluctancy to make rapid control movements. The controller dynamics model consists of an open-loop part which generates the required flight path to be flown as well as the required control inputs to effect the maneuver, and a stabilization part which generates feedback control inputs such that the actual CFT-model-generated flight path tracks the required flight path. In chapter 2 a short description will be given of the helicopter rotor and body dynamic model; chapter 3 will discuss the controller dynamical models, and in chapter 4 an application of the controller, integrated with the CFT-program, will be discussed.

## 2 DYNAMIC MODELS

### 2.1 Helicopter body

The dynamic model of the helicopter body consists of a set of differential equations of motion which, when integrated with respect to time, provides the time histories of all helicopter motion quantities of interest. The equations of motion are non-linear and take into account the rotating mass of the main rotor. Generally the equations can be cast in the following vector form:

$$M(t) \dot{\underline{x}}_t(t) = \underline{f}[\underline{x}_t(t), \underline{u}_t(t), t] \quad (2.1)$$

where the time-varying matrix  $M(t)$  contains the (variable) helicopter mass and inertia moments and products; the state vector  $\underline{x}_t(t)$  describes the total state of the helicopter,  $\underline{u}_t(t)$  is the control vector containing all controls, and  $\underline{f}$  is a complicated vector-valued function containing aerodynamic forces and moments (from rotors and fuselage) and inertia forces and moments, helicopter mass etc. The vector  $\underline{x}_t(t)$  is defined as:

$$\underline{x}_t(t) = [u(t), v(t), w(t), p(t), q(t), r(t), \theta(t), \varphi(t), \psi(t), h(t), x(t), y(t)]^T \quad (2.2)$$

and the control vector  $\underline{u}_t(t)$  as:

$$\underline{u}_t(t) = [\delta_{CP}(t), \delta_a(t), \delta_e(t), \delta_r(t)]^T \quad (2.3)$$

The set of equations (2.1) is generally called the CFT-model. Integration with respect to time using an integration algorithm will yield the time histories  $\underline{x}_t(t)$  of the total helicopter state and the controls  $\underline{u}_t(t)$ .

### 2.2 Main rotor

The dynamic behaviour of the (elastic) rotor is also governed by a set of differential equations, which constitutes the rotor dynamic model. Without derivation the equations are given as follows:

$$q_n''(\psi) + \lambda_n^2 q_n(\psi) = f_n(\psi), \quad n = 1, 2, \dots, k \quad (2.4)$$

where  $f_n(\psi)$  is a complicated aerodynamic forcing function containing blade element aerodynamic and inertia loads as well as modal displacements  $q(\psi)$  and velocities  $\dot{q}_n(t)$  or  $q_n'(\psi)$ , when expressed as function of blade azimuth angle  $\psi$ . A steady-state periodic solution of  $q_n$  is postulated, using constant coefficients:

$$q_n(\psi) = q_{n_o} + q_{n_c} \cos \psi + q_{n_s} \sin \psi, \quad n = 1, 2, \dots, k \quad (2.5)$$

and substituting this into (2.4) yields a set of algebraic equations, from which  $q_{n_o}$ ,  $q_{n_c}$  and  $q_{n_s}$ , for  $n = 1, 2, \dots, k$ , can be solved. This, however, requires a Newton-Raphson-type algorithm to calculate the required variables iteratively. Once calculated, the rotor thrust and hub moments can be determined using numerical integration techniques.

Thus the rotor blade dynamics are assumed to be harmonic, and the entire rotor is behaving in a steady-state manner. This approximation is considered adequate for the present application of the CFT-program.

### 2.3 Trim model

All maneuvers with the CFT-program start from a steady-state, or trim, condition. This may include steady turns and/or climbing or descending flight, including steady-state autorotative flight. Main rotor rpm is not yet a motion variable and is kept at a prescribed value.

The trim model is obtained from eq. (2.1) by requiring:

$$\dot{\underline{x}}_t(t) = \underline{0}$$

which is identical to:

$$\underline{f} [\underline{x}_t(0), \underline{u}_t(0)] = \underline{0} \quad (2.6)$$

The parameters which specify the trim condition are:

aircraft speed  $V$ , height  $h$ , rate of climb ROC, rotor rpm  $\Omega$ , and aircraft mass. These parameters relate to the state vector elements according to the following set of additional trim equations:

$$V = \sqrt{u^2 + w^2} \quad (2.7)(a)$$

$$\text{ROC} = u \sin \theta - w \cos \theta \quad (b)$$

For trim it is furthermore assumed that:

$$v = 0 \quad (2.8)$$

thus zero sideslip is assumed for all trim conditions.

If necessary the state vector  $\underline{x}_t(t)$  may be augmented to include  $\dot{x}$ ,  $\dot{h}$  or  $\dot{y}$ . Equations (2.6), (2.7) and (2.8) together form the augmented trim model with the equations:

$$\underline{g} [\underline{x}_t(0), \underline{u}_t(0)] = \underline{0} \quad (2.9)(a)$$

$$\text{where: } \underline{g} [\underline{x}_t(0), \underline{u}_t(0)] = \begin{pmatrix} \underline{f} [\underline{x}_t(0), \underline{u}_t(0)] \\ V - \sqrt{u^2 + w^2} \\ \text{ROC} - u \sin \theta + w \cos \theta \\ v \end{pmatrix} \quad (b)$$

A modified Newton-Raphson process has been applied to solve eq. (2.9)(a) for the unknown elements of  $\underline{x}_t$  and all the elements of  $\underline{u}_t$ . Because of the important applications of this process later-on, a short description is given in the appendix. In the CFT-program the matrix  $P = [\partial g / \partial \underline{x}_t]$  from eq. (A.7) is calculated and used in the linear(ized) dynamical models employed for the controller. Because  $P$  is calculated for a trim condition, the linearized models are applicable only when the perturbations from trim are such that linearization is allowed.

### 3 CONTROLLER

#### 3.1 General

The controller has been designed to generate control inputs to stabilize the helicopter and to perform maneuvers. The user specifies which motion variables are the primary variables for the maneuver, and which are the "secondary" ones (for stabilization). For example, when one wants to make a pull-up from level flight, the longitudinal motion variables  $u, w, q, \theta, h$  and control  $\delta_e$  (possibly also  $\delta_{CP}$ ) describe the maneuver. If one wants to keep roll angle  $\phi$  constant at its trim value during this maneuver, then one specifies  $\phi$  as a variable for stabilization (or "secondary" variable). There is an almost infinite number of choices which the user can make, but in practice the choice is normally made between subsets of longitudinal variables ( $u, w, q, \theta, x, \delta_{CP}, \delta_e$ ) and lateral/directional variables ( $v, p, r, \phi, \psi, \delta_a, \delta_r$ ). Very often both subsets of variables are used for stabilization, and only one of the two for the maneuver. The number, and type, of maneuvers are only limited by the controllability argument (Ref. 1), which implies that the set of terminal conditions (section 3.3) should be attainable without infinitely large control.

The structure of the controller has been adapted from human pilot models as encountered in human factor analysis. These models are rooted in optimal control and estimation theory and are formulated in the time domain using state space techniques. For the particular application here the display and estimation portions of the human pilot model were omitted since the random noise sources involved in displaying signals and estimating the aircraft state would, in real-time calculations, lead to Monte-Carlo type calculation processes which, by their very nature, consume much computation time. Therefore the controller in the CFT-program may be regarded as a highly motivated, well-trained pilot having no perceptual delays, and having perfect observations of the entire helicopter state. The human pilot models are applicable to linear dynamical systems, hence the requirement to have some scheme with which the respective linear(ized) systems can be derived. This is indicated in the appendix.

#### 3.2 Stabilization model

After the linearization scheme has been applied the controller is to stabilize the following (linear) system:

$$\dot{\underline{x}}_s(t) = A \underline{x}_s(t) + B \underline{u}_s(t) \quad (3.1)$$

where the  $n_{x_s}$ -dimensional vector  $\underline{x}_s(t)$  contains "secondary" variables only, i.e. only those elements of  $\underline{x}_t(t)$  which need stabilization. The  $n_{u_s}$ -dimensional control vector  $\underline{u}_s(t)$  contains only those elements of the total control vector  $\underline{u}_t(t)$  which are specified to be used for stabilization purposes. Both  $\underline{x}_s(t)$  and  $\underline{u}_s(t)$  are vectors whose elements are perturbations of  $\underline{x}_t(t)$  or  $\underline{u}_t(t)$  from the nominally required flight path. The  $(n_{x_s} \times n_{x_s})$ -dimensional (constant) matrix A and  $(n_{x_s} \times n_{u_s})$ -dimensional (constant) matrix B are derived from a linearization scheme as previously outlined.

The initial conditions for the system, eq (3.1), are:

$$\begin{aligned} \underline{x}_s(0) &= \underline{0} \\ \underline{u}_s(0) &= \underline{0} \end{aligned} \quad (3.2)$$

The "feedback", or stabilization control  $\underline{u}_s(t)$ , is required to prevent the helicopter state from deviating from its desired path, that is, to keep  $\underline{x}_s$  "small". This control  $\underline{u}_s(t)$  is generated in such a way that the following quadratic criterion is minimized:

$$J_s = \frac{1}{2} \int_0^{\infty} \left\{ \underline{x}_s^T(t) Q_x \underline{x}_s(t) + \underline{u}_s^T(t) Q_u \underline{u}_s(t) + \dot{\underline{u}}_s^T(t) Q_{\dot{u}} \dot{\underline{u}}_s(t) \right\} dt \quad (3.3)$$

The time derivative of  $\underline{u}_s(t)$  is also weighted, through the term  $\dot{\underline{u}}_s^T(t) Q_{\dot{u}} \dot{\underline{u}}_s(t)$ , in the quadratic cost function  $J_s$ . In human factor analysis terms this weighting reflects pilot's neuro-motor lag<sup>s</sup> or his reluctance to make rapid control movements.

By adjoining  $\dot{\underline{u}}_s$  to the state vector the optimal control  $\underline{u}_s(t)$  which minimizes  $J_s$  while obeying eq. (3.1) can be derived to be (Ref. 2):

$$T_N \dot{\underline{u}}_s(t) + \underline{u}_s(t) = -L \underline{x}_s(t) \quad (3.4)$$

This equation is generally called the "feedback law", where  $T_N$  is a neuro-motor lag matrix, and  $L$  is a constant feedback gain matrix, obtained from solving a Ricatti matrix equation (Ref. 1). It has been assumed that the Ricatti equation has reached a steady-state solution, implying low frequency dynamics compared to system time constants.

The choice of the diagonal weighting matrices  $Q_x$ ,  $Q_u$  and  $Q_{\dot{u}}$  depends upon the objective task requirement and the pilot's subjective mode of behaviour. An often used method is to assume that the weightings are inversely proportional to the square of the maximum allowed deviation, i.e.

$$Q_{x_i} = x_{i,\max}^{-2}$$

where  $x_i$  is the  $i$ -th element of  $\underline{x}_s(t)$ . In accordance with the general practice used in human factor analysis, the weightings of the control and control rate are chosen in a similar fashion; however, the relative weighting is such that the resulting neuro-motor lag time constants are between 0.1 and 0.2 per second.

### 3.3 Flight path generation model

The flight path which the helicopter is desired to follow, is generated also by a linear system of the following form:

$$\dot{\underline{x}}_d(t) = F \underline{x}_d(t) + G \underline{u}_d(t) \quad (3.5)$$

with initial conditions:

$$\underline{x}_d(0) = \underline{x}_{d_0} \quad (3.6)(a)$$

$$\underline{u}_d(0) = \underline{0} \quad (b)$$

here the  $n_{x_d}$ -dimensional vector  $\underline{x}_d(t)$  contains those elements of  $\underline{x}_t(t)$  which are incorporated in performing the maneuver. The  $n_{u_d}$ -dimensional vector  $\underline{u}_d(t)$  contains only those elements of  $\underline{u}_t(t)$  with which the maneuver is to be performed. Both  $\underline{x}_d(t)$  and  $\underline{u}_d(t)$  are vectors whose elements are desired perturbations of  $\underline{x}_t(t)$  from a trimmed steady-state flight path. This is defined by:

$$\underline{x}_{\text{trim}}(t) = \underline{x}_{t_0} + \dot{\underline{x}}_{t_0} \cdot t \quad (3.7)(a)$$

$$\underline{u}_{\text{trim}}(t) = \underline{u}_{t_0} \quad (b)$$

where  $\dot{\underline{x}}_{t_0}$  is a constant vector of time derivatives for trim (e.g. constant sink rate, turn rate at trim, etc.). The  $(n_{x_d} \times n_{x_d})$ -dimensional, time-invariant system dynamics matrix  $F$  and  $(n_{x_d} \times n_{u_d})$ -dimensional, time-invariant control distribution matrix  $G$  are obtained using the previously described linearization scheme around a given trim condition.

In order to take maneuvers into account, aspects of terminal control, or finite time, will have to be taken into consideration. Therefore the control  $\underline{u}_d(t)$  is required to transfer the system, eqs. (3.5) from the given initial condition to a terminal condition at time  $t_f$ , where the following terminal condition has to be met:

$$H \underline{x}_d(t_f) + \underline{c} = \underline{0} \quad (3.8)$$

where  $\underline{c}$  is a constant  $n_{x_f}$ -dimensional vector, given on input by the user, and  $H$  is a constant  $(n_{x_f} \times n_{x_d}^t)$ -dimensional matrix specifying which elements of  $\underline{x}_d(t)$ , or linear combinations thereof, have to meet a terminal condition at time  $t_f$ .

Of the many controls which can accomplish this transfer that one is chosen which minimizes control rate, i.e. minimizes the following cost function:

$$J_d = \frac{1}{2} \int_0^{t_f} \dot{\underline{u}}_d^T(t) Q_{\dot{u}} \dot{\underline{u}}_d(t) dt \quad (3.9)$$

The weighting of control rate in the cost function seems appropriate in view of general piloting techniques. Also in this case it yields a closed-form solution for the control time history  $\underline{u}_d(t)$ . If other terms would have been included in the weighting function of eq. (3.9), complex numerical schemes for solution of  $\underline{u}_d(t)$  would then have become mandatory.

By adjoining the control rate  $\dot{\underline{u}}_d(t)$  to the state vector  $\underline{x}_d(t)$  and solving the optimal control problem of the augmented system, according to reference 1, the resulting optimal control  $\underline{u}_d(t)$  can be shown to be a purely open-loop, or feed-forward, control of the form (Ref. 2):

$$\dot{\underline{u}}_d(t) = -\underline{h}(t) \quad (3.10)$$

where  $\underline{h}(t)$  is described by a vector-differential equation with given terminal boundary condition  $\underline{h}(t_f)$ . Thus, after backward integration with respect to time,  $\underline{u}_d(t)$  is known for  $0 < t < t_f$  and the state  $\underline{x}_d(t)$ , for all  $t$ , can be generated using eqs. (3.5), (3.6) and (3.10) and integrating eq. (3.5) forward with respect to time.

#### 3.4 Integration with helicopter model

The helicopter body dynamic model, also defined as the CFT-model, eq. (2.1), requires the control  $\underline{u}_t(t)$  as input. This control is a summation of the trim value  $\underline{u}_{t_0}$ , the required perturbation  $\underline{u}_d(t)$ , and the stabilization part  $\underline{u}_s(t)$ , as shown in figure 1. The summation applies to corresponding elements of each control vector. Through the non-linear CFT-model the control  $\underline{u}_t(t)$  generates a flight path  $\underline{x}_t(t)$  which is (continuously) compared to the required flight path generated by the flight path generation (FPG-) model, which is  $\underline{x}_d(t) + \underline{x}_{t_0} + \dot{\underline{x}}_{t_0} t$ . The difference between these two flight paths is the stabilization part  $\underline{x}_s(t)$ , which, through proper feedback, generates corrective control inputs  $\underline{u}_s(t)$  so as to drive  $\underline{x}_s(t)$  to zero. The total control  $\underline{u}_t(t)$  is modified by this amount  $\underline{u}_s(t)$ . The complete structure and integration of the

controller is shown in figure 1.

The differences which accrue between actual and desired flight path are due to differences in dynamic model (non-linear versus linearized around a trim condition), time delays in applying corrective control inputs (inherent with the control model), and errors associated with numerical integration algorithms.

#### 4 APPLICATION

As an example of the functioning of the controller to perform a maneuver, and in its role as a stabilizer, two landing flare maneuvers of an Alouette III helicopter have been calculated, both starting from the same initial condition but having different terminal conditions.

The initial condition is a 60 kts descending flight on a  $6^\circ$  glide path (rate of descent 3.2 m/s (633 ft/min)), helicopter mass 1850 kg (4 079 lbs).

The duration of the maneuver is 12 s.

The terminal conditions which apply to both flares are: zero pitch rate ( $\dot{q}=0$ ), zero height ( $h=0$ ) and zero vertical speed ( $\dot{h}=0$ ). In addition to these, the second flare maneuver has a terminal condition on "groundspeed"  $\dot{x}$ , viz.  $\dot{x}(t_f)=15$  m/s (30 kts).

The maneuver is performed primarily using collective pitch and longitudinal cyclic pitch. For stabilization of the longitudinal/lateral variables (section 3.2), excluding  $x$  and  $y$ , all four controls are used.

The desired response of the state variables, as calculated by the FPG-model, is indicated in all figures by a dashed line.

The resulting time-histories are shown in figures 2a-2h. Figure 2<sup>a</sup> shows the time-history of the velocity along the X-axis,  $u(t)$ , for the two flares. It becomes clear that toward the end of the maneuver the difference between desired and actual trace of  $u$  becomes larger due to time delays and increasing non-linearity affects. As might be expected, for the second flare  $u(t_f)$  is lower than for the first flare. The time-histories of the velocity along the Z-axis,  $w(t)$ , is shown in figure 2<sup>b</sup> for the two flares. Clearly there is a larger peak in  $w(t)$ , hence a greater angle of attack, for the second flare, because more deceleration has to take place within the same span of time. Again here, toward the end of the maneuver, a greater discrepancy has developed between desired and actually calculated response, this discrepancy being larger for the second flare because of stronger non-linearity effects (greater departure from trim) and because of time delay effects, which will become more apparent when "quicker" maneuvering is required.

Figure 2<sup>c</sup> shows the response of pitch rate, and pitch angle in figure 2<sup>d</sup>. Clearly a larger pitch-up maneuver is required for the second flare so as to allow for a stronger deceleration. The same arguments as before apply to the discrepancies between desired and actually calculated response. For these reasons also the pitch rate did not meet the prescribed terminal condition.

In figure 2<sup>e</sup> is shown height versus time and height rate of change (vertical speed or climb rate) versus time is shown in figure 2<sup>f</sup>. Due to time delays and non-linearity effects the aircraft undershoots its terminal condition for the second flare. Also the time duration of the maneuver has been a little too much, because the desired trace of height, for the second flare, shows a "dip" at around 7 s from the start. This implies that, in order to minimize control rate during the flare, the controller uses the phugoid oscillation to advantage, such that the terminal condition is met with minimum control effort indeed. The desired path only has to meet terminal conditions; there are no "intermediate" conditions given, e.g. to remain clear of the ground before final time. It is therefore well possible that the desired path, especially for long-term maneuvers close to the ground, may reach below zero height conditions before the final time. The control response, to perform the flares, is given in figures 2<sup>g</sup> and 2<sup>h</sup>.

For both flares the control inputs are very mild and small changes are enough to bring the maneuver about.

For the second flare, the collective is reduced slightly and aircraft deceleration is therefore achieved by flaring, or pitching up. Obviously, more aft cyclic is required for the greater pitch-up in the second flare, as illustrated by figure 2<sup>h</sup>.

## 5 CONCLUDING REMARKS

For a computer-flight-testing program for helicopters, the generation of control inputs to perform a maneuver has greatly been facilitated by the incorporation of a controller. This consists of two models i.e. a flight path generation model (FPG) and a stabilization model (STAB). Because of the multiple options available, a highly flexible tool has become available, which has not yet been fully explored. Both models in conjunction performed well to execute flare maneuvers.

For the FPG-model, the terminal conditions could have been modified so as to have the aircraft meet the terminal conditions exactly. For maneuvers of long duration, say more than 10-15 s, specifying only a terminal condition and weighting only control rate may not be adequate to describe the entire open-loop maneuver. Further work in this area is required. The stabilization part can be updated more frequently, so as to have feedback gains optimized for the locally linearized system. This will reduce discrepancies between desired and actually calculated response due to non-linearity effects.

## 6 REFERENCES

1. Bryson Jr., A.E.  
Ho, Yu- Chi  
Applied optimal control-optimization, estimation, and control.  
Ginn and Company, Waltham, Mass., 1969.
2. Kleinman, D.L.  
Killingsworth, W.R.  
A predictive pilot model for STOL aircraft landing.  
NASA CR-2374, March 1974.

## ACKNOWLEDGEMENT

This paper is based on work done under contract for the Directorate of Materiel Air of the Royal Netherlands Air Force. The author wishes to express his gratitude for their permission to publish these results.

APPENDIX

Trim algorithm and linearization

When starting the Newton-Raphson algorithm to find the unknowns for a particular trim condition, an estimate is made of the augmented state vector  $\hat{\underline{x}}_t(0)$ , where:

$$\hat{\underline{x}}_t(0) = [\underline{x}_t(0), \underline{u}_t(0)]^T \quad (A.1)$$

Then an initial estimate is  $\hat{\underline{x}}_t$ , where it is assumed that:

$$\hat{\underline{x}}_t = \hat{\underline{x}}_t(0) + \Delta \hat{\underline{x}}_t \quad (A.2)$$

where  $\hat{\underline{x}}_t(0)$  is the true solution of eq. (2.9)(a).

Generally, when substituting  $\hat{\underline{x}}_t$  in (2.9) one has:

$$\underline{g}[\hat{\underline{x}}_t] \neq \underline{0}$$

but is approximately close to  $\underline{0}$ . A linearized Taylor series expansion yields:

$$\begin{aligned} \underline{g}[\hat{\underline{x}}_t] &\stackrel{\Delta}{=} \underline{g}[\hat{\underline{x}}_t(0) + \Delta \hat{\underline{x}}_t] \\ &= \underline{g}[\hat{\underline{x}}_t(0)] + \{\partial \underline{g}[\hat{\underline{x}}_t(0)]/\partial \hat{\underline{x}}_t\} \cdot \Delta \hat{\underline{x}}_t + \dots \end{aligned} \quad (A.3)$$

Because  $\underline{g}[\hat{\underline{x}}_t(0)] = \underline{0}$  eq. (A.3) results in:

$$\underline{g}[\hat{\underline{x}}_t] = [\partial \underline{g}/\partial \hat{\underline{x}}_t] \Delta \hat{\underline{x}}_t \quad (A.4)$$

where  $[\partial \underline{g}/\partial \hat{\underline{x}}_t]$  is written instead of  $\{\partial \underline{g}[\hat{\underline{x}}_t(0)]/\partial \hat{\underline{x}}_t\}$ . From this equation  $\Delta \hat{\underline{x}}_t$  may be solved:

$$\Delta \hat{\underline{x}}_t = [\partial \underline{g}/\partial \hat{\underline{x}}_t]^{-1} \cdot \underline{g}[\hat{\underline{x}}_t] \quad (A.5)$$

and a subsequent, improved guess of the true trim value of  $\hat{\underline{x}}_t(0)$  can be calculated, using eq. (A.2) as algorithm:

$$\hat{\underline{x}}_t(0) = \hat{\underline{x}}_t - \Delta \hat{\underline{x}}_t$$

or:

$$\hat{\underline{x}}_t \text{ new} = \hat{\underline{x}}_t \text{ old} - \Delta \hat{\underline{x}}_t \quad (A.6)$$

This process continues until  $\underline{g}[\hat{\underline{x}}_t \text{ new}] \approx \underline{0}$  with sufficient accuracy. During this process the matrix  $\partial \underline{g}/\partial \hat{\underline{x}}_t$  is calculated (numerically), where, using eq. (A.1):

$$[\partial \underline{g}/\partial \hat{\underline{x}}_t] = [\partial \underline{g}/\partial \underline{x}_t \quad | \quad \partial \underline{g}/\partial \underline{u}_t] \quad (A.7)$$

The sub-matrices  $\partial \underline{g}/\partial \underline{x}_t$  and  $\partial \underline{g}/\partial \underline{u}_t$  can be used directly in the linearization of the dynamical equations around a trim condition. Linearizing eq. (2.1) around a trim condition  $\underline{x}_t(0)$ ,  $\underline{u}_t(0)$  yields:

$$\begin{aligned} M_0 \Delta \dot{\underline{x}}_t(t) &= [\partial f\{\underline{x}_t(0), \underline{u}_t(0)\}/\partial \underline{x}_t] \Delta \underline{x}_t(t) \\ &\quad + [\partial f\{\underline{x}_t(0), \underline{u}_t(0), 0\}/\partial \underline{u}_t] \Delta \underline{u}_t(t) \end{aligned} \quad (A.8)$$

In matrix form:

$$\Delta \dot{\underline{x}}_{\underline{t}}(t) = A \Delta \underline{x}_{\underline{t}} + B \Delta \underline{u}_{\underline{t}}(t) \quad (\text{A.9})$$

where matrices A and B equate directly to  $M_0^{-1}[\partial \underline{f} / \partial \underline{x}_{\underline{t}}]$  and  $M_0^{-1}[\partial \underline{f} / \partial \underline{u}_{\underline{t}}]$  respectively. Because of the relation between vector  $\underline{g}$  and  $\underline{f}$  in equation (2.9)(b) it is obvious that when  $\partial \underline{g} / \partial \underline{x}_{\underline{t}}$  and  $\partial \underline{g} / \partial \underline{u}_{\underline{t}}$  are calculated during the Newton-Raphson process, also the matrices A and B from eq. (A.9) can be derived.

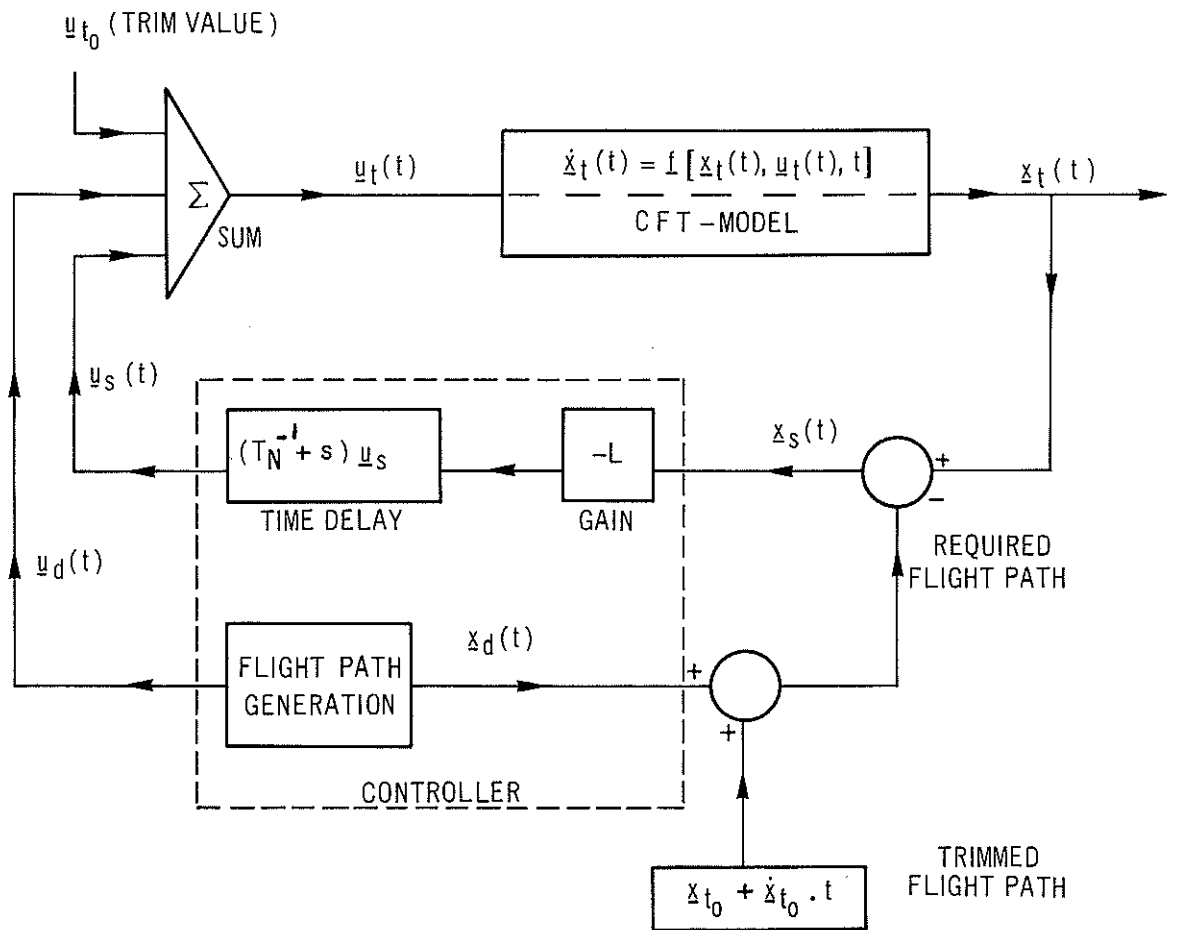


Fig. 1 Operational scheme of controller, combined with the CFT-model

HELICOPTER NAME	ALOUETTE III
WEIGHT	18142 N (1849 KGF)
ALTITUDE	15 m ( 50 FT )
FLIGHT SPEED	30.9 m/s ( 60 KTS)
CENTER OF GRAVITY LOCATION (AFT OF DATUM)	2.95 m (116.1INCH)

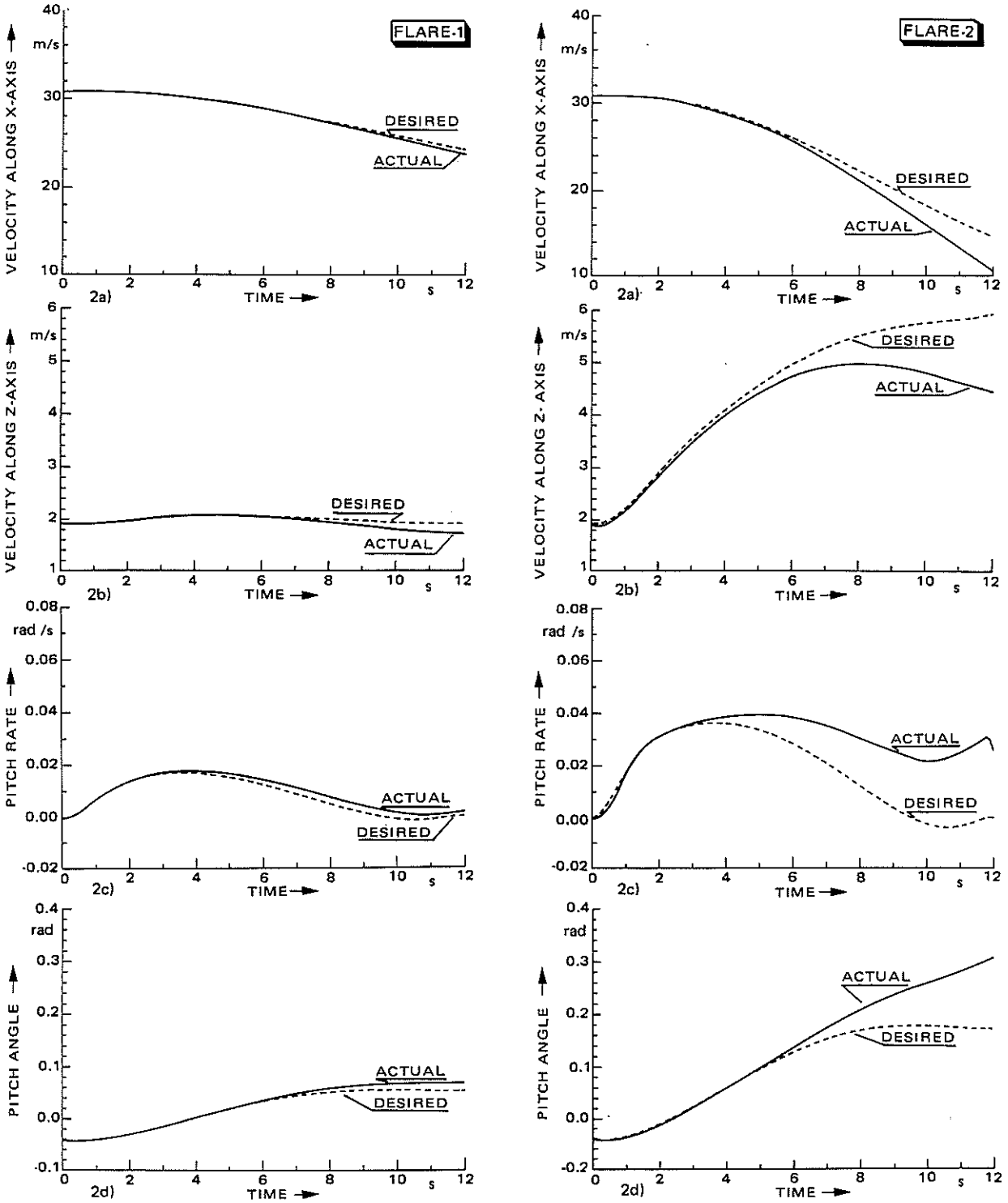


Fig. 2 Response of helicopter during two flares

HELICOPTER NAME	ALOUETTE III
WEIGHT	18142 N (1849 KGF)
ALTITUDE	15 m ( 50 FT )
FLIGHT SPEED	30.9 m/s ( 60 KTS)
CENTER OF GRAVITY LOCATION (AFT OF DATUM)	2.95 m (116.1 INCH)

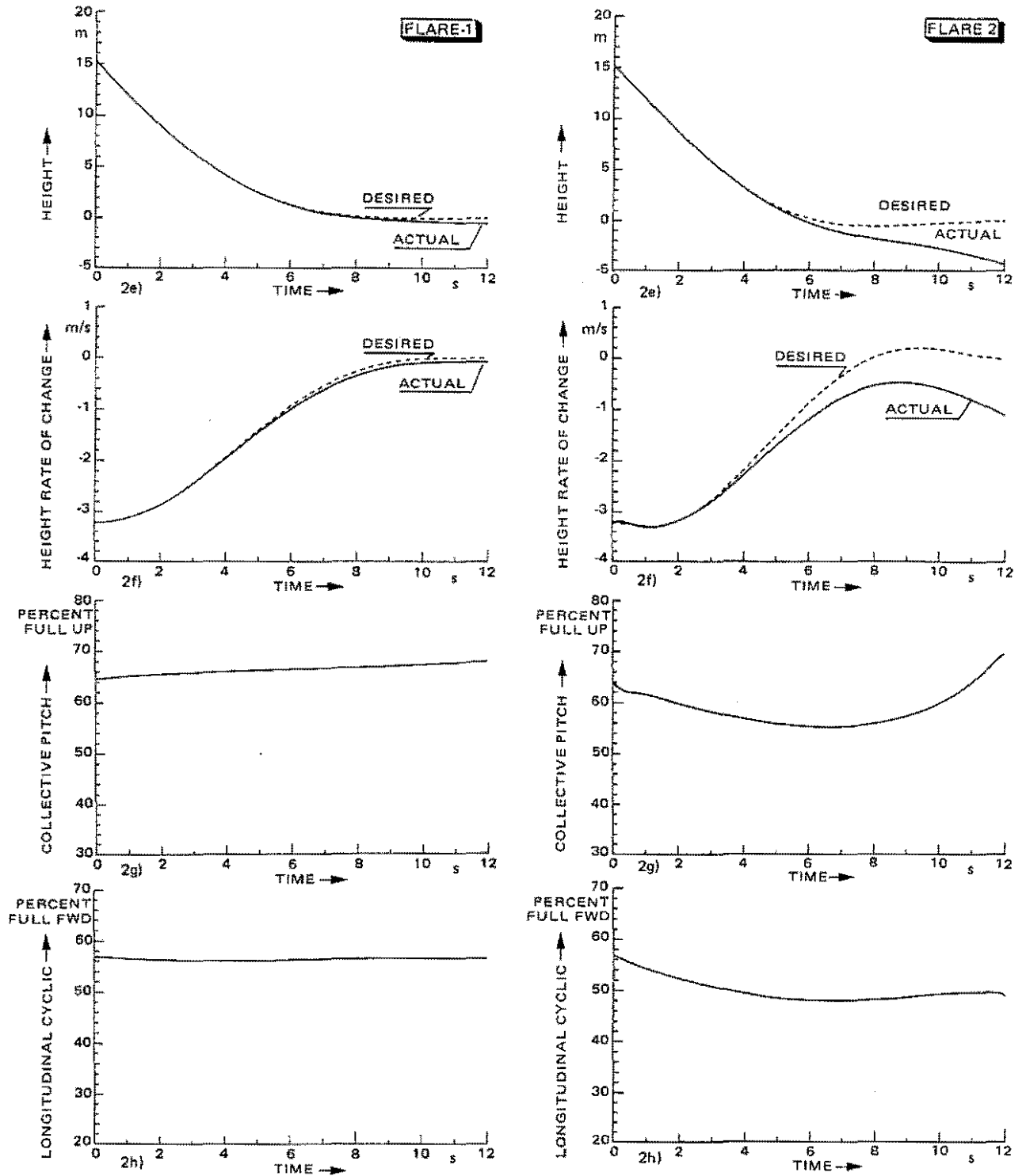


Fig. 2 Continued